Acta Oceanol. Sin., 2023, Vol. 42, No. 2, P. 142–149
https://doi.org/10.1007/s13131-022-2112-3
http://www.aosocean.com
E-mail: ocean2@hyxb.org.cn

Spatial and temporal variation process of seabed dynamic response induced by the internal solitary wave

Zhuangcai Tian[1, 2*], Lei Jia[1], Naili Hu[3], Susheng Wang[1], Mingwei Zhang[1*], Guoqing Zhou[1]

[1] State Key Laboratory for Geomechanics and Deep Underground Engineering, China University of Mining and Technology, Xuzhou 221116, China

[2] Key Laboratory of Coastal Science and Integrated Management, Ministry of Natural Resources, Qingdao 266061, China

[3] Shandong Provincial Key Laboratory of Marine Environment and Geological Engineering, Ocean University of China, Qingdao 266100, China

Received 1 January 2022; accepted 18 July 2022

Abstract

Internal solitary wave (ISW) is often accompanied by huge energy transport, which will change the pore water pressure in the seabed. Based on the two-dimensional Biot consolidation theory, the excess pore water pressure in seabed was simulated, and the spatiotemporal distribution characteristics of excess pore water pressure was studied. As the parameters of both ISW and seabed can affect the excess pore water pressure, the distribution of pore water pressure showed both dissipation and phase lag. And parametric studies were done on these two phenomena. Due to influenced by the phase lag of excess pore water pressure, the penetration depth under the site of northern South China Sea with total water depth 327 m, induced by typical internal solitary wave increased by 26.19%, 53.27% and 149.86% from T_0 to $T_{0.5}$ in sand silt, clayey silt and fine sand seabed, respectively. That means the effect of ISW on seabed will be underestimated if we only take into accout the penetration depth under ISW trough, especially for fine sand seabed. In addition, the concept of "amplitude-depth ratio" had been introduced to describe the influence of ISW on seabed dynamic response in the actual marine environment. In present study, it is negatively correlated with the excess pore water pressure, and an ISW with smaller amplitude-depth ratio can wide the range of lateral impacts. Our study results help understand the seabed damage induced by the interaction between ISW and seabed.

Key words: internal solitary wave, pore water pressure, seabed, dynamic response, variation process

Citation: Tian Zhuangcai, Jia Lei, Hu Naili, Wang Susheng, Zhang Mingwei, Zhou Guoqing. 2023. Spatial and temporal variation process of seabed dynamic response induced by the internal solitary wave. Acta Oceanologica Sinica, 42(2): 142–149, doi: 10.1007/s13131-022-2112-3

1 Introduction

Internal solitary wave (ISW), mainly generated by strong winds, tides, and currents, is a special nonlinear internal wave in the density stratified ocean. And it is widely distributed in the global ocean, such as the both sides of the Atlantic Ocean, the west bank of the Pacific Ocean, the coast of the Indian Ocean and the South China Sea (Jackson, 2007; Zhang et al., 2020; Lü et al., 2021). The observation of Huang et al. (2016) showed that the largest amplitude of ISW was up to 240 m. That means a strong water disturbance occuring when the ISW is passing. Also, sediment re-suspension, sand waves (a dynamic rhythmic bed form), sedimentary waves (a ripple topography formed by the resuspended sediment deposit), and scoured channels will be formed. In the areas with more obvious topographic fluctuations, such as submarine canyons, the effect of ISW is more obvious (Alford et al., 2015; Tian et al., 2019b, c, 2021a). Chen et al. (2012) suggested that ISW was also the important factors inducing submarine landslides. And *in-situ* observations had found that ISW can exert forces on the seabed and induces the dynamic response to the seabed, which in turn affects the stability of the seabed (Thomas et al., 2016).

Unlike surface waves, ISW usually has large amplitudes and wavelengths, which could cause significant bottom current and pressure backflow and interact with the seabed (Duda et al., 2004). Chen and Hsu (2005) is the first to conduct a simulation study on the change of seabed pore water pressure caused by ISW. They used an eigenvalue problem to solve the wave pressure on seabed surface caused by ISW and solved the pore water pressure in the seabed with infinite depths as well as the sediment displacement. Then, Williams and Jeng (2007) adopted the same method to calculate pore water pressure. In addition, their study paid attention to the attenuation of internal waves that induced by the interaction with seabed. Zhao et al. (2016) simulated seabed liquefaction caused by a solitary wave. Rivera-Rosario et al. (2017) established a two-layer water model and calculated the velocity and density fields by solving the Dubreil-Jacotin-Long equation. The results showed that poor conductive seabed was more likely to be damaged, and ISW was more likely to induce seabed damage when the seawater depth was within 100 m.

Foundation item: The Natural Science Foundation of Jiangsu Province under contract No. BK20210527; the Open Research Fund of Key Laboratory of Coastal Science and Integrated Management, Ministry of Natural Resources under contract No. 2021COSIMQ002; the National Natural Science Foundation of China under contract No. 42107158.
*Corresponding author, E-mail: zhuangcaitian@163.com; meiichiyou@gmail.com

Based on the two-layer stratified fluid system and 2-D Biot theory, Qiao et al. (2016) conducted a parameter study on pore water pressure induced by ISW, including the permeability, shear modulus, porosity and saturation of seabed. Su et al. (2017) calculated three cases with common sediments on the northern continental slope of the South China Sea, and found that shear failure and residual liquefaction would not occur under the action of ISW, and transient liquefaction may only occur at shallow depths (z=–0.35 m). However, both Qiao et al. (2016) and Su et al. (2017) pay more attention to the macro impact, and lack investigation on the distribution of pore pressure. Tian et al. (2019a) analyzed the pore water pressure and penetration depth caused by ISW based on laboratory experiment and numerical simulation. In their study, the vertical distribution of pore water pressure in sandy silt and clayey silt was similar, and the penetration depth of sandy silt was greater than that of clayey silt. The vertical distribution of pore pressure also related to the phase of ISW (Rivera-Rosario et al., 2017; Tian et al., 2019a). However, these studies paid attention to the stability of seabed, and there is few study on the distribution of pore water pressure, especially the horizontal distribution. In present study, the distribution characteristcs of pore water pressure was studied, and the time effect was also considered, which is important for in-depth understanding and prediction of ISW-induced geological hazards.

Referring to the models of Chen and Hsu (2005), Qiao et al. (2016), and Tian et al. (2019a), this paper conducted a simulation using relevant parameters extracted from field observation. The study reveals the variation trend of pore water pressure in the seabed during the action of an ISW, as well as the spatial and temporal variation of pore water pressure in the vertical and horizontal directions. The results will provide a reference for theoretical analysis and *in-situ* observation of pore water pressure changes caused by ISW.

2 Numerical model

The ISW-seabed numerical model established in this study is shown in Fig. 1. It is a two-layer fluid system structure for simulating the horizontal movement of the ISW. The ISW with wavelength L, the half of wavelength Lw, and amplitude A is also showen in Fig. 1. And the upper layer with thickness h_1 and density ρ_1 was lighter than the lower layer with thickness h_2 and density ρ_2.

The pressure associated with the free-surface displacement has little influence when the water depth is greater than 100 m (Rivera-Rosario et al., 2017). Thus the effect of surface waves was neglected in this study, as well as the viscosity and rotation of seawater (Chen and Hsu, 2005). The ISW moved forward only in one direction without considering its attenuation. The seabed was an isotropic and homogeneous porous structure. Pore water in the seabed could be compressed, and its seepage followed Darcy's law. And the interface between the lower fluid and the seabed was regarded as a wall surface. Based on two-dimensional Biot consolidation theory, the excess pore water pressure in seabed caused by ISW is calculated.

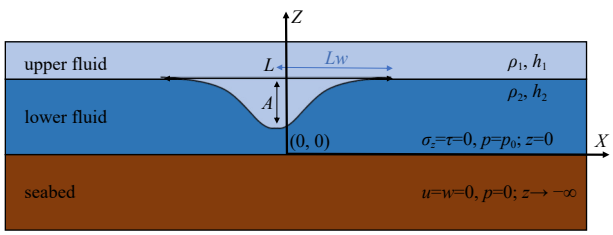

Fig. 1. Schematic diagram of the simulation system for seabed pore water pressure induced by internal solitary wave.

2.1 *Action of ISW*

According to the equation sorted out by Qiao et al. (2016), the motion equation of the ISW surface at the interface of two layers of seawater was

$$\eta(x,t)=\begin{cases}0, & t\in(0,T/4)\cup(3T/4,T)\\ A\mathrm{e}^{\mathrm{i}(kx-\omega t)}, & t\in[T/4,3T/4]\end{cases}, \tag{1}$$

where t is time, i is imaginary unit, k is the wavenumber ($k=2\pi/L$), and ω is the angular frequency ($\omega=2\pi/T$).

The lower velocity potential of a fluid system is a function of horizontal and vertical coordinates x, y, and time t, defined as $\varphi(x,z,t)$. The velocity potential in the fluid layer follows the Laplace equation. The wave pressure resulting from an ISW at any point in the flow field of the lower seawater is P,

$$P=\rho\frac{\partial\varphi(x,z,t)}{\partial t}, \tag{2}$$

where ρ is density of fluid.

According to initial conditions and boundary value such as velocity potential and wave motion equation, when $t\in[T/4, 3T/4]$, the hydrodynamic pressure generated by ISW at the seabed surface (namely, the vertical coordinate z=0) is expressed in Eq. (3) (Chen and Hsu, 2005; Qiao et al., 2016),

$$\begin{aligned}p_0=&-\frac{\mathrm{i}\rho_w A}{k\rho_2}\times\\ &\left\{\begin{aligned}&\frac{-gk\rho_2\omega^2\cosh kh_1+\left[g^2k^2(\rho_2-\rho_1)+\rho_1\omega^4\right]\sinh kh_1}{gk\sinh kh_1-\omega^2\cosh kh_1}\cosh kh_2\\ &+\frac{\rho_2\omega^4\cosh kh_1-gk\rho_2\omega^2\sinh kh_1}{gk\sinh kh_1-\omega^2\cosh kh_1}\sinh kh_2\end{aligned}\right\}\times\\ &\mathrm{re}\left\{\mathrm{e}^{\mathrm{i}(kx-\omega t)}\right\},\end{aligned} \tag{3}$$

where ρ_w is reference fluid density, A is the amplitude of ISW, k is wave number, ω is angular frequency, re is the real part of the function, i is an imaginary unit, and g is the acceleration of gravity.

2.2 *Seabed model*

According to the two-dimensional Biot consolidation theory summarized by Chen and Hsu (2005) and Tian et al. (2019a), the general equation of pore water pressure in the seabed is

$$K_x\frac{\partial^2 p}{\partial x^2}+K_z\frac{\partial^2 p}{\partial z^2}-\gamma_w n\beta\frac{\partial p}{\partial t}=\gamma_w\frac{\partial\varepsilon}{\partial t}, \tag{4}$$

where p is the wave-induced excess pore water pressure, K_x is the permeability coefficient of sediment in the x direction, K_z is the permeability coefficient of sediment in the z direction, γ_w is the bulk density of pore water, n is the porosity of sediment, β is the compression coefficient of pore fluid, and ε is volumetric strain. ε includes displacement in x and z directions,

$$\varepsilon=\frac{\partial u}{\partial x}+\frac{\partial w}{\partial z}, \tag{5}$$

where u and w are the displacement of sediment in the x and z directions, respectively.

In the seabed sediment model, σ_x and σ_z represent the effective stress of sediment in x and z directions, respectively, and τ represents the shear stress. According to the two-dimensional Biot consolidation theory, the equilibrium equation of force in two dimensions is as follows:

$$\begin{cases} \dfrac{\partial \sigma_x}{\partial x} + \dfrac{\partial \tau}{\partial z} = \dfrac{\partial p}{\partial x}, \\ \dfrac{\partial \tau}{\partial x} + \dfrac{\partial \sigma_z}{\partial z} = \dfrac{\partial p}{\partial z}. \end{cases} \tag{6}$$

The specific derivation process can refer to the work of Chen and Hsu (2005) and Qiao et al. (2016). Here, the analytical equation similar to that established by Hsu et al. (1993) for solving the hydrodynamic pressure and displacement of the seabed is directly given as follows:

$$u = p_0 \left[-\left(C_0 + C_1 z\right) \mathrm{e}^{kz} + C_2 \mathrm{e}^{\delta z} \right] \mathrm{e}^{\mathrm{i}(kx-\omega t)} , \tag{7}$$

$$w = p_0 \left\{ \left[-\mathrm{i}C_0 - \mathrm{i}C_1 z + \frac{(1+2\lambda)}{k} \mathrm{i}C_1 \right] \mathrm{e}^{kz} - \frac{\delta}{k} \mathrm{i}C_2 \mathrm{e}^{\delta z} \right\} \mathrm{e}^{\mathrm{i}(kx-\omega t)} , \tag{8}$$

$$p = \left\{ p_0 - \frac{2G\left(1-2\mu-\lambda\right)}{\left(1-2\mu\right)} \mathrm{i}C_1 \mathrm{e}^{kz} + \frac{2G\left(1-2\mu\right)\left(k^2-\delta^2\right)}{\left(1-2\mu\right)k} \mathrm{i}C_2 \mathrm{e}^{\delta z} \right\} \mathrm{e}^{\mathrm{i}(kx-\omega t)}, \tag{9}$$

where C_0, C_1, and C_2 are undetermined coefficients, δ and λ are correlation coefficients with sediment and wave.

2.3 *ISW and seabed sediment parameters*

The relevant parameters of ISW were selected from the observation in the Liuhua Sea of the South China Sea (Table 1; Duda et al., 2004). According to the study of Luan et al. (2012), the sediment types of the simulated seabed were fine sand, sandy silt, and clayey silt classified by Shepard method, which were widely distributed in the northern South China Sea. The strength parameters of surficial sediment should be important to the calculation results (Guo et al., 2022a, b), so the specific physical and mechanical property parameters of these sediments were collected from the research data of Sino-German SO(SONNE)95 voyage in 1994, SO72A voyage in 1990, HY4-20 121 voyage of Guangzhou Marine Geological Survey in 2012 (Lu, 1996; Zhou et al., 2020). Mechanical parameters of similar sediments were used to supply some parameters that *in-situ* data could not be found. The sorted parameters were given in detail in Table 2.

3 Results

ISW drives the movement of the upper and lower seawater to form a wave pressure on the top surface of seabed, which induces the seepage of pore water in seabed (Tian et al., 2022), and forms excess pore water pressure. Accordingly, the distribution of effective stress in the seabed will be changed. When the effective stress reached the threshold value, the seabed sediment will lose its original strength and be deformed and destroyed. Some studies focused on seabed damage induced by ISW had conducted (Su et al., 2017; Rivera-Rosario et al., 2017; Tian et al., 2021b). Then we paid more attention to the detailed variation of pore pressure in seabed, providing a reference to the observation of pore pressure in deep-sea.

3.1 *Model validation*

In order to verify the accuracy of the model, we adopted the same working conditions as Qiao et al. (2016), and simulated the excess pore water pressure curve. The comparation is shown in Fig. 2. Saturation had a significant influence on the vertical distribution of excess pore water pressure. At same depth, the greater was the saturation of the seabed, the greater was the excess pore water pressure. The present results were consistent with Qiao et al. (2016).

3.2 *Vertical distribution of pore water pressure*

In this section, the parameters of ISW1 in Table 1 had been used to calculate the pore water pressure in seabed. T_0 was defined as the time when the ISW trough located on the monitored section. T is the period of ISW. Then five moments had been selected, namely $T_{-0.2}$=T_0–0.2T, T_0, $T_{0.1}$=T_0+0.1T, $T_{0.2}$=T_0+0.2T, $T_{0.5}$=T_0+0.5T. The results had been treated as dimensionless. The vertical coordinate y (y=10×z/Lw) is the relative depth, and the horizontal coordinate x (x=P/p_0) is the ratio of excess pore water pressure to maximum wave pressure, where P is the excess pore water pressure, and p_0 is the maximum wave pressure. It should be noted that the pore pressure caused by depression ISW is negative, and absolute values are used to compare sizes in this paper.

The vertical distribution of pore water pressure caused by ISW at position x=0, including five moments, is shown in Fig. 3. At the moments $T_{-0.2}$, T_0, $T_{0.1}$, the ratio of the excess pore water pressure decreased rapidly to a stable value with depth in all three sediment (Figs 3a–c), but the corresponding depth is not same. For clayey silt seabed, the stable value occurs at 10z/Lw= –0.25. The result in sand silt seabed is similar with that of clayey silt. But it needs a deeper depth for pore pressure in fine sand to reach a stable vauel, and the relative depth (10z/Lw) is about –0.50.

Table 1. Parameters of internal solitary wave (ISW) in the northern South China Sea

Parameters	Upper fluid thickness h_1/m	Lower fluid thickness h_2/m	Upper fluid density ρ_1/(kg·m^{-3})	Lower fluid density ρ_2/(kg·m^{-3})	Amplitude A/m	Period T/s
ISW1	112	215	1 022.5	1 025.5	80.9	1 440
ISW2	40	300	1 022.5	1 025.5	165	840

Table 2. Surface layer sediment properties of the northern slope of the South China Sea

Type	Shear modulus G/Pa	Permeability k/(m·s^{-1})	Poisson's ratio/ μm	Pore water bulk density γ_w/(kN·m^{-3})	Porosity n	Saturation Sr
Fine sand	1×10^7	5×10^{-6}	0.33	10 260	0.541	1 or 0.98, in present study Sr=0.98
Sandy silt	1×10^7	1×10^{-6}	0.31	10 260	0.717	1 or 0.98, in present study Sr=0.98
Clayey silt	1.48×10^7	3.47×10^{-7}	0.31	10 260	0.753	1 or 0.98, in present study Sr=0.98

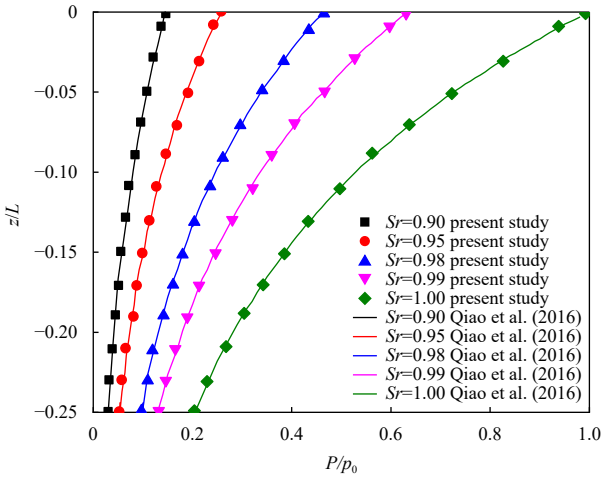

Fig. 2. Comparison of present simulation and results of the literature (Qiao et al., 2016). Symbols were results of the present paper, solid lines were results of the literature (Qiao et al., 2016).

Then, at the moments $T_{0.2}$ and $T_{0.5}$ (Figs 3d, e), the ratio of the excess pore water pressure increases firstly at a shallow surface and then decreases rapidly with the depth. When t=$T_{0.2}$, the peak value occurs with the relative depth 0.02, 0.02, 0.09 for sand silt, clayey silt and fine sand seabed respectively. And when t=$T_{0.5}$, the peak value occurs with the relative depth 0.09, 0.16 and 0.38 for sand silt, clayey silt and fine sand seabed, respectively. There are also differences between the stable points. The stable values of P/p_0 in sand silt and clayey silt seabed are tending to 0, but it is tending to –0.10 in fine sand seabed.

3.3 *Horizontal distribution of pore water pressure*

Horizontally, the ratio of excess pore water pressure presented a similar distribution in three kinds sediment for all depth (Figs 4a–c). It is largest at the middle position and rapidly decreases to both sides. And it decreases with the depth. It is worth noting that the curve with a large depth generally falls to the left of that with a small depth, which indicated that there is a phase lag in dynamic response in seabed. In Fig. 4d, the peak values of each curve in Figs 4a–c are presented. Obviously, fine sand seabed has the largest peak (P/p_0=–0.49), sand silt seabed was second (P/p_0=–0.46), and clayey silt seabed was the smallest (P/p_0=–0.42). And we can evaluate the degree of phase lag by the horizontal distance between adjacent peak points. Then, it shows the phase lag in clayey silt seabed is most obvious, sand silt seabed is second, and fine sand seabed has a lower phase lag.

3.4 *Seabed response under different ISWs*

The vertical distribution of pore pressure induced by the two ISWs shows similar changes (Fig. 5). The ratio of the excess pore water pressure decreases with depth at the moment t=$T_{-0.2}$, T_0, and $T_{0.1}$, and increases firstly and then decreases with depth at $T_{0.2}$ and $T_{0.5}$. And the ratio of the excess pore water pressure caused by ISW1 in the seabed is slightly larger than that caused by ISW2 at the same depth.

As shown in Fig. 6, the excess pore water pressure induced by the two ISWs both present a U-shaped horizontal distribution with large in the middle and small on both sides. In the beginning, at z=–0.2 m (Fig. 6a), the ratios of the excess pore water pressure caused by the two ISWs are significantly different only in the range of –0.5< x/Lw< 0.5, and the maximum difference is about 0.02. When z=–0.4 m, it has a significant difference in the range of –0.7< x/Lw<0.8, and the maximum difference (about 0.04) is larger than z=–0.2 m. The difference continued to enlarge with depth until z=–0.1 m , where the obvious difference between two curves in the range of –1.2<x/Lw<1.8. And the maximum difference is about 0.07.

4 Discussion

4.1 *Dissipation and phase lag of pore water pressure*

In the problem of wave-seabed intereaction, most studies consider the surface of seabed as a drainage boundary (Zhao et al., 2016; Rong et al., 2019), which means the wave pressure can change the pore pressure in the surface of seabed directly. Then the change will transfer vertically and horizontally, which is

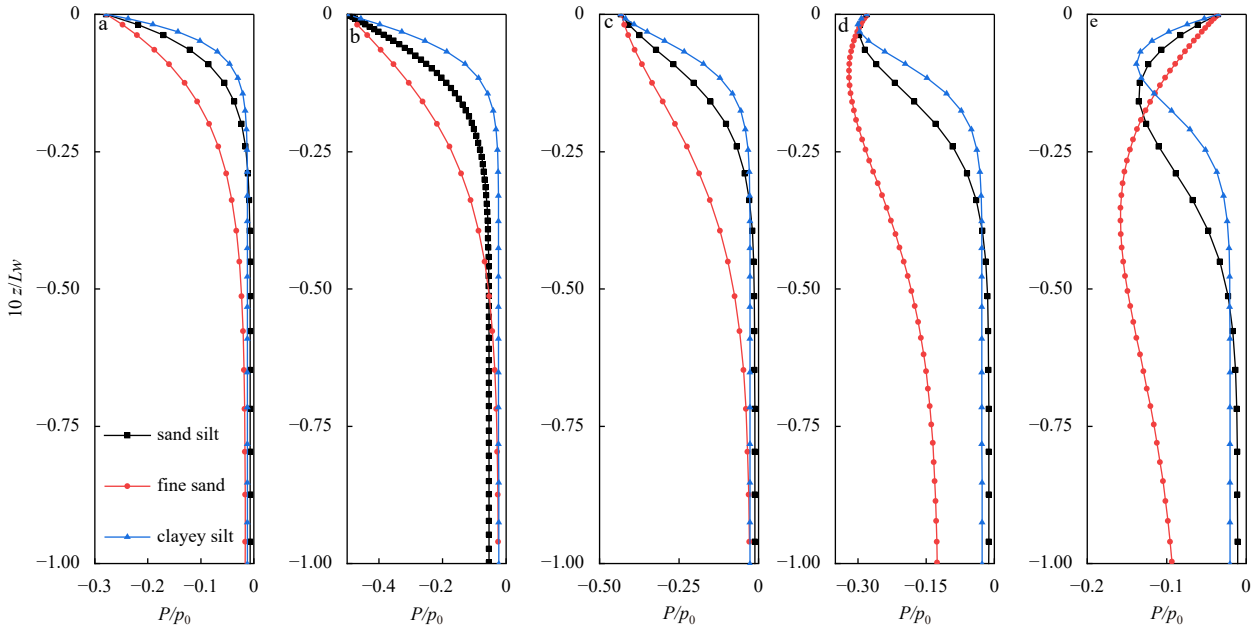

Fig. 3. Vertical distribution of excess pore pressure in sandy silt seabed under the action of ISW1. a. $T_{-0.2}$; b. T_0; c. $T_{0.1}$; d. $T_{0.2}$; e. $T_{0.5}$.

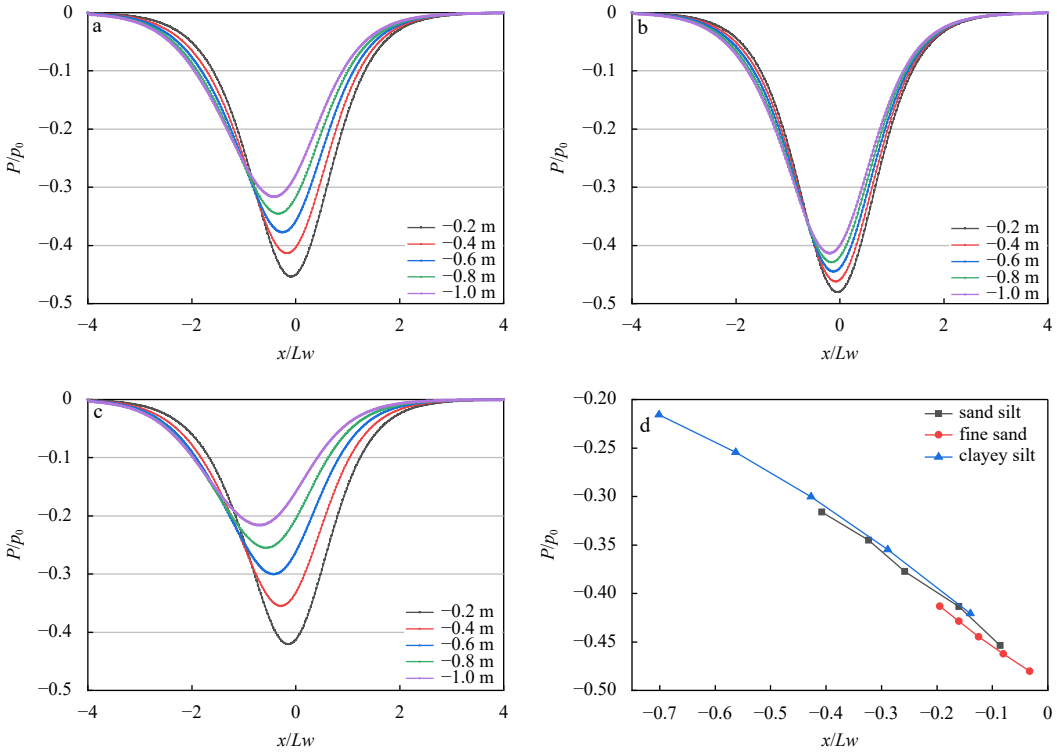

Fig. 4. Horizontal distribution of excess pore water pressure under the action of ISW1 at t=T_0. a. Sand silt seabed; b. fine sand seabed; c. clayey silt seabed; d. summary of peak values in each curve.

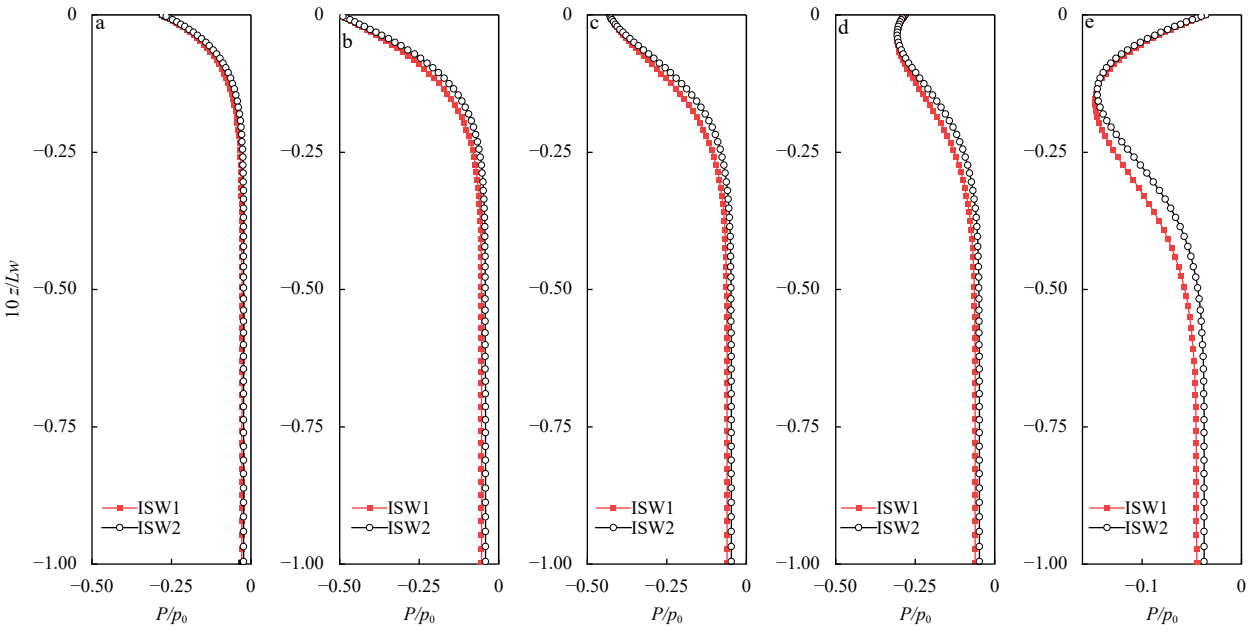

Fig. 5. Vertical distribution of excess pore water pressure in sandy silt seabed under different ISWs. a. $T_{-0.2}$; b. T_0; c. $T_{0.1}$; d. $T_{0.2}$; e. $T_{0.5}$.

studied in this paper. In the present results, the vertical distribution of pore water pressure (Fig. 3) is similar to the study of Rivera-Rosario et al. (2017). And the horizontal distribution of pore water pressure (Fig. 4) shows a similar "U" shape to the results of Qiao et al. (2018) in the flume experiment. The impact on seabed induced by ISW is a dynamic process, and the transient variation of pore water pressure in seabed should be focused. And in present study, the distribution of pore water pressure in seabed shows both dissipation and phase lag. The dissipation is expressed the reduction of peak pore water pressure in the whole interaction. While the phase lag means that the peak value occurs a little later in a deeper position. Then the parametric studies are used to investigate the dissipation and phase lag in seabed (Fig. 7), including shear modulus, permeability, Poisson's ratio and porosity.

In Fig. 7, the time history curves of pore water pressure in five depths were draw firstly, but only the peak values were kept in present graph. And these five points in one curve are located

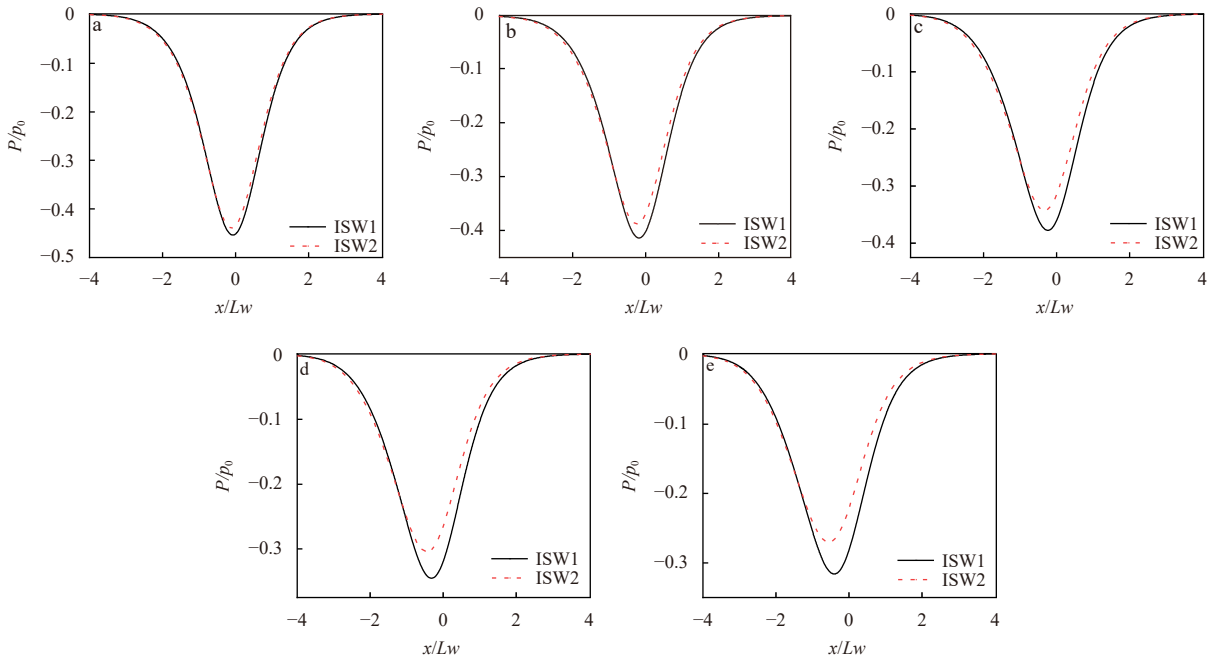

Fig. 6. Horizontal distribution of excess pore water pressure in sandy silt seabed under different ISWs. a. z=–0.2 m; b. z=–0.4 m; c. z=–0.6 m; d. z=–0.8 m; e. z=–1.0 m.

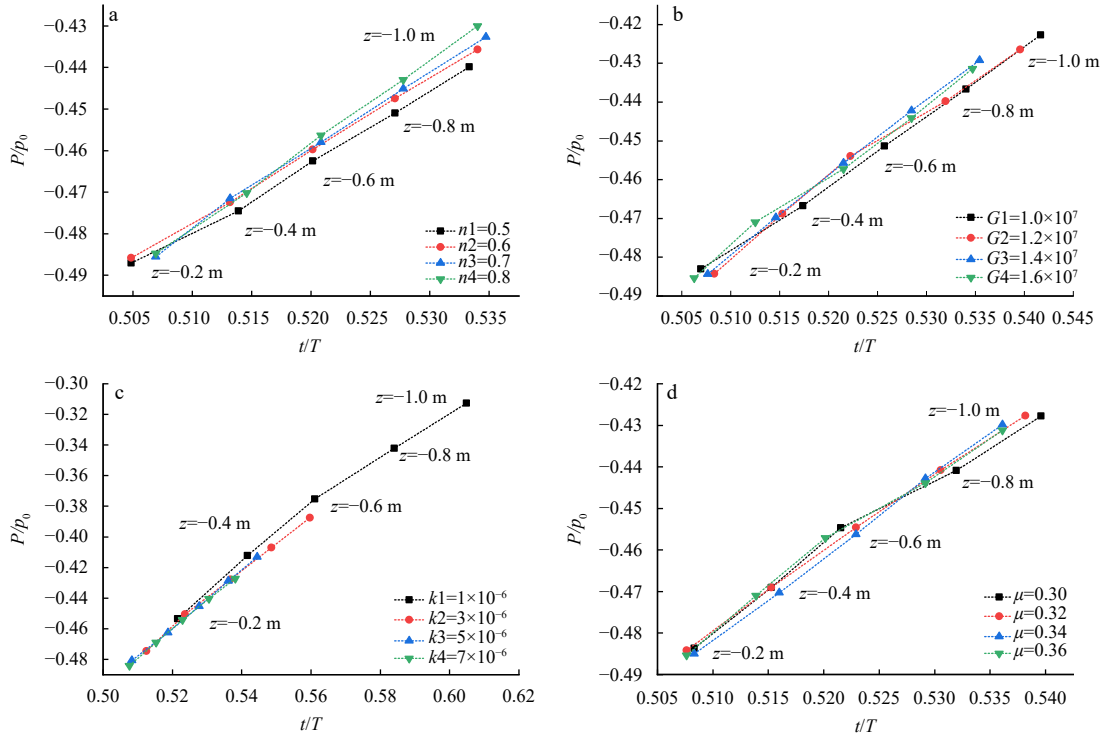

Fig. 7. The effects of porosity (n), shear modulus (G), permeability (k) and Poisson's ratio (μ) on the dissipation and phase lag of excess pore water pressure (peak value) induced by ISW1. a. Various porosity; b. various shear modulus; c. various permeability; d. various Poisson's ratio.

z=–0.2 m, z=–0.4 m, z=–0.6 m, z=–0.8 m and z=–1.0 m from left to right, respectively. For two adjacent points on the same curve, their vertical difference can reflect the dissipation of pore water pressure, and the horizontal difference can mirror the phase lag. In Fig. 7a, the values of P/p_0 are close in four cases with z=–0.2 m, but shows differences with the depth gradually. The greater is the porosity, the more is pore pressure dissipation, which indicated that poroisty has a positive effect on the dissipation of pore water pressure. But there is no obvious law of phase lag horizontally. Figure 7b shows that both dissipation and phase lag of pore water pressure reduce slightly with the increase of shear modulus. Permeability also shows a negative effect, and it has more obvi-

ous influence than shear modulus (Fig. 7c). However, there are just a little differences vertically between the four cases (Fig. 7d), and the rule of phase lag is not clear, which is not enough to estimate the effect of Poisson's ratio on these two phenomena.

4.2 *Amplitude-depth ratio*

Wave parameters also play an important role in the response of pore water pressure in seabed. Chen and Hsu (2005) showed that pore pressure was related to the wave cycle. Rong et al. (2019) pointed out that wave amplitude would directly affect the wave pressure, and wave cycle would change the wave pressure on the seabed surface by affecting the wavelength. However, an actual ISW may have both the smaller amplitude and longer period, such as two ISWs in Table 1, it is difficult to compare the influence on the seabed response between two actual ISWs by controlling variables. Amplitude and lower water depth are two key parameters of ISW. Therefore, the concept of "amplitude-depth ratio" has been proposed in this paper, and is defined as the ratio of ISW amplitude to the lower water depth. According to this definition, the response of pore water pressure induced by ISW can be qualitatively described.

The amplitude-depth ratio of ISW1 was A/h_2=80.9/215=0.376, and the ratio of ISW2 was 0.550. By the results, ISW1 with a small amplitude-depth ratio has a larger ratio of excess pore water pressure at the same depth than ISW2. Also a smaller amplitude-depth ratio has a larger lateral range of influence, and the difference will enlarge with the depth.

However, only two groups of measured ISW data were used for comparison in this study. Therefore, these conclusions could not sufficiently reveal the generality of the effect of amplitude-depth ratio on seabed response. In the future, a large number of data comparisons are needed to determine the influence of this ratio on seabed response, which will be helpful to evaluate the impact induced by ISW on the seabed in the actual marine environment.

4.3 *Penetration depth*

Jeng and Cha (2003) numerically calculated the pore water pressure in the porous seabed induced by nonlinear waves. Their results showed that the ratio of the excess pore water pressure was larger in the seabed with higher saturation. Based on this result, it was speculated that excess pore water pressure induced by nonlinear waves would penetrate deeper in the seabed with high saturation. Olsthoorn et al. (2012) pointed out that the penetration depth of internal waves with long wavelengths was larger than that of surface waves. And it was positively correlated with wavelength.

In previous studies, the penetration depth was defined as the critical depth at which the change of excess pore water pressure at the trough was 10% of the minimum pressure induced by the ISW (Rivera-Rosario et al., 2017; Tian et al., 2019a). Because the seepage of pore water was not obvious in the sediment within the depth range of $|P|/p_0$< 0.1.

The distribution of pore water pressure both in present study and Rivera-Rosario et al. (2017) shows the characteristics of vertical distribution varies in the whole process. Further, because there is a phase lag when the pore pressure is transferred down, the excess pore water pressure can not reach the peak value immediately in a deeper position under the ISW trough. Therefore, the caculation with t=T_0 as the typical value of penetration depth is not enough. Thus more time nodes ($T_{-0.2}$, T_0, $T_{0.1}$, $T_{0.2}$, $T_{0.5}$) had been selected to investigate the penetration depth in present study. Figure 8 shows the penetration depth in three kinds of

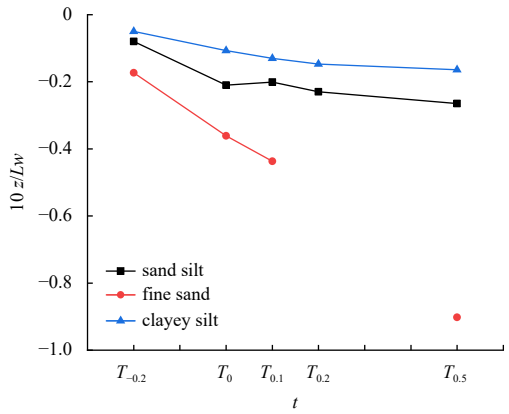

Fig. 8. The penetration depth in various sediment induced by ISW1 at t=$T_{-0.2}$, T_0, $T_{0.1}$, $T_{0.2}$ and $T_{0.5}$.

seabed at five moments. The value of P/p_0 is close to but not the threshold value, so the penetration depth in fine sand seabed at t=$T_{0.2}$ is not given to the curve. The penetration depth in clayey silt, sand silt and fine sand seabed increases in turn, which partly consist with Tian et al. (2019a). However, the penetration depth under ISW trough (t=T_0) is not maximum, but increases gradually with time. Especially for fine sand seabed, the penetration depth under the site of northern South China Sea with total water depth 327 m, induced by typical internal solitary wave is about $10z/Lw$=–0.36 at t=T_0, but increase significantly to –0.92 at t=$T_{0.5}$. Under the same water conditions, the penetration depth increased by 26.19%, 53.27% and 149.86% from T_0 to $T_{0.5}$ in sand silt, clayey silt and fine sand seabed, respectively.

Combining wave-current loading, Qi et al. (2019) showing that the wave-induced pore pressure was increased for the following-current case, but reduced for the opposing-current case. In the actual seabed environment, the penetration depth of the wave-induced pore pressure in the seabed was closely related to the wave's parameters, motion, evolution, and seabed properties. Similarly, the evolution process of the ISW should also be considered when studying the penetration depth of ISW in the future.

5 Conclusions

In present study, a two-layer and stratified fluid system and an seabed model based on Biot consolidation were established to investigate the spatial and temporal variation of excess pore water pressure in seabed induced by ISW. And some conslusions are summerized:

(1) Due to the dissipation and phase lag of pore water pressure in seabed, both vertical and horizontal distribution of excess pore water pressure are related to the phase of ISW. Porosity can promote the dissipation, while shear modulus and permeability have a negative impact on both the dissipation and phase lag.

(2) The ISW with smaller amplitude-depth ratio can cause a larger excess pore water pressure and wider horizontal distribution range. And the effect will be enlarged with depth.

(3) The three kinds of sediments simulated in this paper, the penetration depth in clayey silt, sand silt and fine sand seabed increases in turn. And the amplitude-depth ratio of ISW is negatively correlated with the penetration depth. Influenced by the phase lag of excess pore water pressure, the penetration depth under the site of northern South China Sea with total water depth 327 m, induced by typical internal solitary wave increased by 26.19%, 53.27% and 149.86% from T_0 to $T_{0.5}$ in sand silt, clayey silt and fine sand seabed, respectively. Clearly, the effect of ISW on

seabed will be underestimate if we only take into accout the penetration depth at $t=T_0$, especially for fine sand seabed.

The paper is limited to discuss the horizontal seabed model, while the breaking phenomenon of ISW propagating over inclined seabed will result in a new distribution of pore pressure. Therefore, the distribution of pore pressure induced by ISW in inclined seabed should be studied in the future to compare their correlation and difference, providing more basis for the theoretical analysis of seabed dynamic response.

References

Alford M H, Peacock T, Mackinnon J A, et al. 2015. The formation and fate of internal waves in the South China Sea. Nature, 521(7550): 65–69, doi: 10.1038/nature14399

Chen Chengyi, Hsu J R C. 2005. Interaction between internal waves and a permeable seabed. Ocean Engineering, 32(5–6): 587–621

Chen Shanshan, Sun Yunbao, Wu Shiguo. 2012. Sea bottom landslide in the Shenhu area on the north margin of South China sea and triggering mechanisms. Marine Geology Letters (in Chinese), 28(6): 40–45

Duda T F, Lynch J F, Irish J D, et al. 2004. Internal tide and nonlinear internal wave behavior at the continental slope in the northern South China Sea. IEEE Journal of Oceanic Engineering, 29(4): 1105–1130, doi: 10.1109/JOE.2004.836998

Guo Xingsen, Nian Tingkai, Wang Dong, et al. 2022a. Evaluation of undrained shear strength of surficial marine clays using ball penetration-based CFD modelling. Acta Geotechnica, 17(5): 1627–1643, doi: 10.1007/s11440-021-01347-x

Guo Xingsen, Nian Tingkai, Zhao Wei, et al. 2022b. Centrifuge experiment on the penetration test for evaluating undrained strength of deep-sea surface soils. International Journal of Mining Science and Technology, 32(2): 363–373, doi: 10.1016/j.ijmst.2021.12.005

Hsu J R C, Jeng D S, Tsai C P. 1993. Short-crested wave-induced soil response in a porous seabed of infinite thickness. International Journal for Numerical and Analytical Methods in Geomechanics, 17(8): 55–576

Huang Xiaodong, Chen Zhaohui, Zhao Wei, et al. 2016. An extreme internal solitary wave event observed in the northern South China Sea. Scientific Reports, 6(1): 30041, doi: 10.1038/srep30041

Jackson C. 2007. Internal wave detection using the Moderate Resolution Imaging Spectroradiometer (MODIS). Journal of Geophysical Research: Oceans, 112(C11): C11012, doi: 10.1029/2007JC004220

Jeng D S, Cha D H. 2003. Effects of dynamic soil behavior and wave non-linearity on the wave-induced pore pressure and effective stresses in porous seabed. Ocean Engineering, 30(16): 2065–2089, doi: 10.1016/S0029-8018(03)00070-2

Lü Haibin, Liu Yujun, Chen Xiaokang, et al. 2021. Effects of westward shoaling pycnocline on characteristics and energetics of internal solitary wave in the Luzon Strait by numerical simulations. Acta Oceanologica Sinica, 40(5): 20–29, doi: 10.1007/s13131-021-1808-0

Lu Bo. 1996. Study on sediments and their physical properties in Dongsha Islands. Haiyang Xuebao (in Chinese), 18(6): 82–89

Luan Xiwu, Sun Dianqi, Peng Xuechao. 2012. Genesis of the nanbeiwei shoal on the shelf of the northern South China Sea and its petroliferous significance. Haiyang Xuebao (in Chinese), 86(4): 626–640

Olsthoorn J, Stastna M, Soontiens N. 2012. Fluid circulation and seepage in lake sediment due to propagating and trapped internal waves. Water Resources Research, 48(11): W11520

Qi Wengang, Li Changfei, Jeng Dongsheng, et al. 2019. Combined wave-current induced excess pore-pressure in a sandy seabed: Flume observations and comparisons with theoretical models. Coastal Engineering, 147: 89–98, doi: 10.1016/j.coastaleng.2019.02.006

Qiao Luzheng, Guo Xiujun, Tian Zhuangcai, et al. 2016. Analysis on internal solitary wave-induced dynamic response characteristics of surface sediments in the northern South China Sea. Chinese Journal of Underground Space and Engineering (in Chinese), 12(S2): 604–611

Qiao Luzheng, Guo Xiujun, Tian Zhuangcai, et al. 2018. Experimental analysis of pore pressure characteristics of slope sediments by shoaling internal solitary waves. Haiyang Xuebao (in Chinese), 40(1): 68–76

Rivera-Rosario G A, Diamessis P J, Jenkins J T. 2017. Bed failure induced by internal solitary waves. Journal of Geophysical Research: Oceans, 122(7): 5468–5485, doi: 10.1002/2017JC012935

Rong Fu, Liao Chencong, Tong Dagui, et al. 2019. Analysis of wave-induced liquefaction of seabed with variation in permeability anisotropy. Journal of Shanghai Jiao Tong University (in Chinese), 53(1): 93–99

Su Yuxi, Qiao Luzheng, Guo Xiujun, et al. 2017. Analysis of internal solitary wave-induced seabed stability of sediments in the northern South China Sea. Geotechnical Investigation & Surveying, 45(11): 30–36

Thomas J A, Lerczak J A, Moum J N. 2016. Horizontal variability of high-frequency nonlinear internal waves in Massachusetts Bay detected by an array of seafloor pressure sensors. Journal of Geophysical Research: Oceans, 121(8): 5587–5607, doi: 10.1002/2016JC011866

Tian Zhuangcai, Chen Tian, Yu Le, et al. 2019a. Penetration depth of the dynamic response of seabed induced by internal solitary waves. Applied Ocean Research, 90: 101867, doi: 10.1016/j.apor.2019.101867

Tian Zhuangcai, Jia Yonggang, Chen Jiangxin, et al. 2021a. Internal solitary waves induced deep-water nepheloid layers and seafloor geomorphic changes on the continental slope of the northern South China Sea. Physics of Fluids, 33(5): 053312, doi: 10.1063/5.0045124

Tian Zhuangcai, Jia Yonggang, Du Qizhi, et al. 2021b. Shearing stress of shoaling internal solitary waves over the slope. Ocean Engineering, 241: 110046, doi: 10.1016/j.oceaneng.2021.110046

Tian Zhuangcai, Jia Yonggang, Zhang Shaotong, et al. 2019b. Bottom and intermediate nepheloid layer induced by shoaling internal solitary waves: impacts of the angle of the wave group velocity vector and slope gradients. Journal of Geophysical Research: Oceans, 124(8): 5686–5699, doi: 10.1029/2018JC014721

Tian Zhuangcai, Liu C, Ren Z, et al. 2022. Impact of seepage flow on sediment resuspension by internal solitary waves: parameterization and mechanism. Journal of Oceanology and Limnology, doi: 10.1007/s00343-022-2001-9

Tian Zhuangcai, Zhang Shaotong, Guo Xiujun, et al. 2019c. Experimental investigation of sediment dynamics in response to breaking high-frequency internal solitary wave packets over a steep slope. Journal of Marine Systems, 199: 103191 doi: 10.1016/j.jmarsys.2019.103191

Williams S J, Jeng D S. 2007. The effects of a porous-elastic seabed on interfacial wave propagation. Ocean Engineering, 34(13): 1818–1831, doi: 10.1016/j.oceaneng.2007.02.002

Zhang Xudong, Zhang Jie, Meng Junmin, et al. 2020. Observation of internal waves with OLCI and SRAL on board Sentinel-3. Acta Oceanologica Sinica, 39(3): 56–62, doi: 10.1007/s13131-019-1510-7

Zhao Hongyi, Jeng Dongsheng, Zhang Huijie, et al. 2016. 2-D integrated numerical modeling for the potential of solitary wave-induced residual liquefaction over a sloping porous seabed. Journal of Ocean Engineering and Marine Energy, 2(1): 1–18, doi: 10.1007/s40722-015-0033-3

Zhou Qingjie, Li Xishuang, Liu Lejun, et al. 2020. Physical properties of the seabed inversed based on Chirp data and the Biot-Stoll model in the northern continental slope of the South China Sea. Haiyang Xuebao (in Chinese), 42(3): 72–82